NASA TECHNICAL NOTE

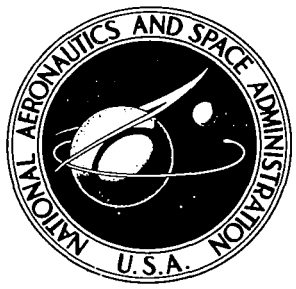

LIGHT-DETECTION ELECTRONICS FOR A RAMAN LIDAR

by Robert J. Leser and Jack A. Salzman

Lewis Research Center
Cleveland, Ohio 44135

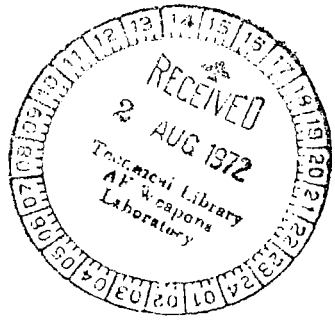

NATIONAL AERONAUTICS AND SPACE ADMINISTRATION • WASHINGTON, D. C. • JULY 1972

1. Report No.	2. Government Accession No.	3. Recipient's Catalog No.
NASA TN D-6879		

4. Title and Subtitle	5. Report Date
LIGHT-DETECTION ELECTRONICS FOR A RAMAN LIDAR	July 1972
	6. Performing Organization Code

7. Author(s)	8. Performing Organization Report No.
Robert J. Leser and Jack A. Salzman	E-6864
	10. Work Unit No. 113-31

9. Performing Organization Name and Address	11. Contract or Grant No.
Lewis Research Center National Aeronautics and Space Administration Cleveland, Ohio 44135	
	13. Type of Report and Period Covered: Technical Note

12. Sponsoring Agency Name and Address	14. Sponsoring Agency Code
National Aeronautics and Space Administration Washington, D.C. 20546	

15. Supplementary Notes

16. Abstract

A light-detection system for an optical radar, or lidar, unit to be used for remote temperature and composition measurements was designed, built, and bench tested. This detection system processes three return signal wavelengths: two Raman wavelengths, and the Rayleigh-Mie wavelength at 694.3 nanometers. Means of coping with photomultiplier tube instabilities and limitations are discussed. Circuits for gain control, ranging, and digitizing are included. The phototube gains can be switched fully on in 80 meters (540 nsec) or off in 30 meters (200 nsec) of range. The range circuit processes signals from 0.1 to 2 kilometers, with an estimated range resolution of less than 5 meters.

17. Key Words (Suggested by Author(s))	18. Distribution Statement
Lidar Light-detection Raman Photomultiplier tube Laser	Unclassied - unlimited

19. Security Classif. (of this report)	20. Security Classif. (of this page)	21. No. of Pages	22. Price*
Unclassified	Unclassified	28	$3.00

* For sale by the National Technical Information Service, Springfield, Virginia 22151

LIGHT-DETECTION ELECTRONICS FOR A RAMAN LIDAR

by Robert J. Leser and Jack A. Salzman

Lewis Research Center

SUMMARY

The purpose of this work was to develop a light-detection system for a Raman lidar unit. Circuits were developed for gain control of the photomultiplier tubes, ranging, and digitizing functions. Test circuits were included for checking the background light signal and the gain balance of the Raman signal channels. Tests of the completed detection system using simulated signals indicate that, at maximum gain, 2.5 digital counts are recorded for every photon in the Raman channels. The system operates over a range of 0.1 to 2 kilometers, with an estimated resolution of 4.7 meters.

INTRODUCTION

The use of a laser as a remote sensing probe appears to have promising potential in a variety of applications. By utilizing the laser as an optical radar device (lidar) whose return signal results from the backscattering of the light by gas molecules, a number of atmospheric parameters can be measured (ref. 1). Investigators have used the elastically backscattered light from a laser beam to remotely observe atmospheric variables such as aerosol or particulate concentration levels (refs. 2 and 3). Lidar techniques have also been successfully employed by using inelastic Raman scattering to identify a number of atmospheric constituents and possible pollutants (refs. 4 to 6). Utilization of the Raman return of a lidar system to remotely measure local atmospheric temperatures has been proposed by Cooney (ref. 7) and Pressman (ref. 8) and has been shown to be a feasible measurement technique through Lewis Research Center laboratory experiments (ref. 9). This technique involves simultaneously monitoring at least two portions of the Raman return signal from a major atmospheric constituent and examining the ratios of their intensities.

A Raman lidar system was designed to demonstrate its capabilities as a remote temperature-monitoring device. The system was designed to operate on a test range where the temperature of the target atmosphere could be controlled and monitored. A

major portion of the design study in this work involved the electronic techniques for the receiver unit, which must collect and measure the low-level Raman return signal. Early lidar systems have used an analog technique - an oscilloscope display of the photomultiplier tube output current. The oscilloscope display was recorded on either a storage oscilloscope or high-speed polaroid film for data acquisition (ref. 10). While this method is adequate for many diagnostic measurements, it does not provide the data in a tractable form for the accurate ratio computations needed for temperature determinations. Photon counting has been suggested as an alternate method of handling the return signal for some lidar operations (ref. 11). This technique is more efficient and provides for both digital counting and storage, but it can only be used for very low-level signals, where the time resolution of the detector will allow counting all the individual pulses. If the signal level is low enough to utilize photon counting, it is generally not amenable to accurate temperature measurements.

This report presents the results of a design study on the receiver electronics in a lidar system. The receiver design is a hybrid of the analog system used in early lidars and the digital photon counter technique. The combination is successful in this short-range system. Circuit designs are presented which solve the system and component problems, and bench test data of the assembled electronics are discussed. The function of these electronics is to detect, condition, and display two discrete components of a laser-Raman back-scattered light signal. In addition to the normal requirements placed on lidar electronics, this system was also designed to operate on a test range with limited boundaries. The system samples one discrete range segment during each test shot. Bench test data with simulated signals have been employed to verify the integrity of the design.

LIDAR SYSTEM

Optical Design

A schematic of the Lewis Research Center optical radar, or lidar, system is shown in figure 1. This system is intended to remotely gather data on gas temperature and composition by utilizing Raman scattering. The system is designed for short-range applications and daylight operation. Specific goals are a minimum range of about 100 meters and a range resolution of 10 meters. The transmitter is a Q-switched ruby laser with an output wavelength of 694.3 nanometers. The output pulse width is 20 nanoseconds, and the output energy is 4 joules per pulse at the rate of 10 pulses per minute. Light scattered from the gas target is gathered by a 25.4-centimeter reflecting telescope and is spectrally analyzed at three wavelengths (two selected Raman wavelengths, and

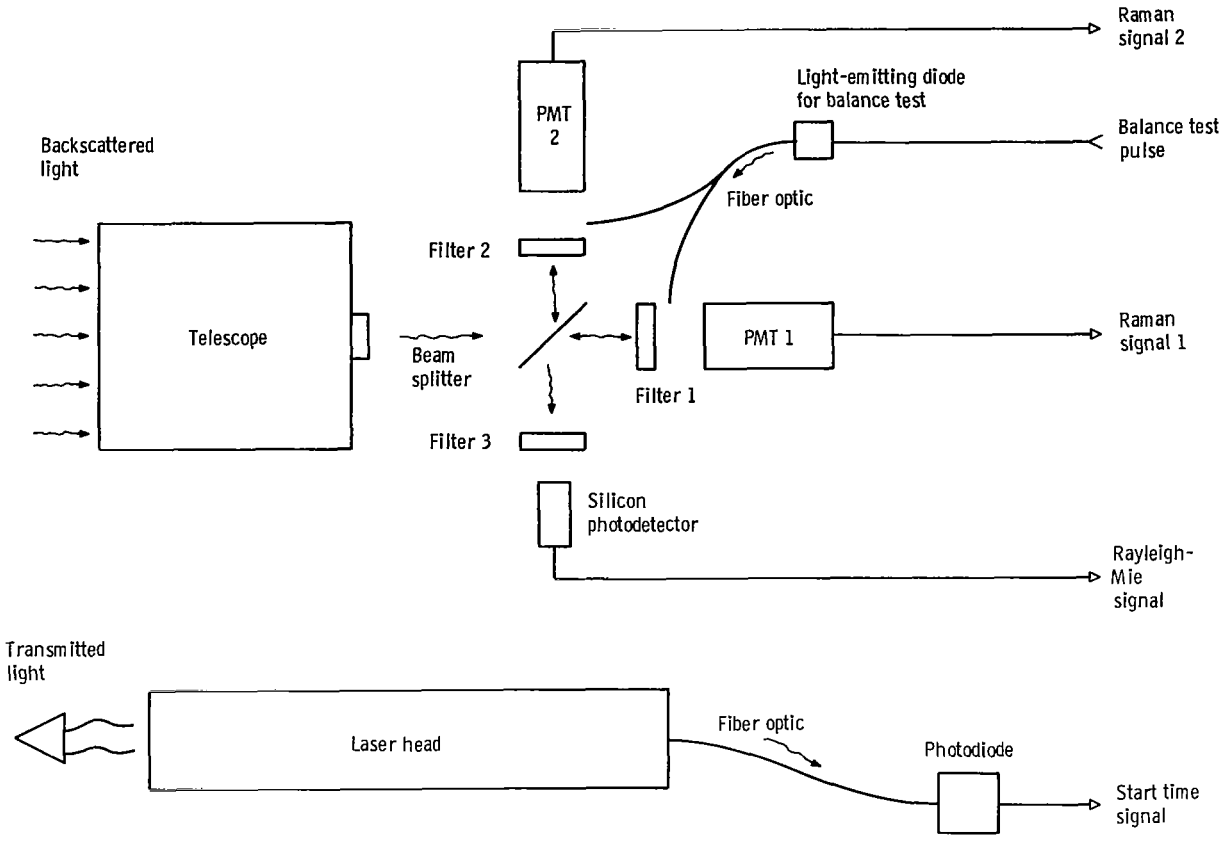

Figure 1. - Optical design schematic.

the Rayleigh-Mie component at 694. 3 nm). A beam splitter at the output of the telescope distributes the return, or back-scattered light, to filter 1 and photomultiplier tube (PMT) 1 for one Raman signal, to filter 2 and PMT 2 for the second Raman signal, and to filter 3 and a silicon photodetector for the Rayleigh-Mie signal. Gas temperature and composition are functions of the ratios of the Raman and Rayleigh signals (ref. 9).

Electronic Design Considerations

The system design considerations are PMT characteristics, background light, system calibration, range resolution, and the output data format. Specific design considerations for the photomultiplier tubes are overload, response time, current gain stability, and power supply voltage stability.

Photomultiplier tube. - The photomultiplier tube can be overloaded by light scattered from very short ranges. The PMT has very slow recovery characteristics, and optical overloads result in short-term instabilities and "after-pulsing" (ref. 12). After-pulsing is the occurrence of spontaneous electrical pulses out of the PMT that appear a short time after apparent recovery from optical overloads. The phenomenon has not been explained. In addition, overloading a PMT shortens the life of the tube due to wearout of the dynodes and aging of the cathode. Thus, some form of PMT overload protection is mandatory.

Mechanical shutters are effective in preventing overload, but their response characteristics are too slow for short-range lidar systems. Commercially available electro-optical modulators, such as a Pockels cell, can be used as shutters; but they are rather leaky and result in a significant loss in signal (i. e., greater than 50 percent loss). Electrical pulsing of the PMT voltages seems to be the best available means of protecting against overload and was selected for this purpose in our design. A pulsing technique developed by the Stanford Research Institute (ref. 13) operates the PMT at very low gain until the potential overload time is over. A pulse is then applied to the PMT, increasing the gain to its normal high value. Although some after-pulsing may still appear when using this scheme, its effects on the system operation are apparently quite repeatable and can possibly be suppressed further during actual field operations (ref. 13). In our design, the Stanford scheme was also used with another circuit to force equally fast turnoff times of the PMT gain. This fast turnoff, or tailgate, avoids possible overloads from high return signals caused by undesired objects in the receiver field of view at ranges beyond the sampled region. For example, in this study, quick turnoff was necessitated by the boundaries of the test range.

A second important design consideration for circuits using photomultiplier tubes is the stability of the current gain. Since the magnitude of the PMT current is a measure of the intensity of the Raman signal, the PMT current gain must be stable for any quantitative measurements. (In our system, the relative stabilization of the ratio of gains of the two PMT's is more important than stabilizing the absolute gains.) Thus, gain stabilization measures are necessary, and the following measures were incorporated in the electronic design: Since the gain of a PMT is temperature dependent, the temperature differential between the two PMT's is stabilized by insulation and instrumented for continuous monitoring. Voltage sensitivity is another PMT shortcoming, but this can be minimized with well-regulated power supplies. The voltage for both PMT's is taken from a single supply to avoid possible gain changes.

Background light. - Background light is a major problem in daylight lidar operation. A high-power, short-pulse laser was selected so that the expected Raman return would greatly exceed the normal daylight, clear-sky background in the spectral region of interest. However, the short pulse duration precludes the use of state-of-the-art photon

counter systems. For this system, a photon counter would have to be capable of at least 10-gigahertz count rates. So in this design the PMT's operate as analog light-to-current converters rather than as photon counters.

Diagnostic tests. - The PMT gain stability and the background light problem necessitate some method of calibration. Incorporated in this design are provisions for automatically checking the system's operation. These include the "background test" and "balance test." A background test was incorporated which is a combined PMT and background intensity check occurring 1/2 second after each laser shot. For this background test the receiver is operated without the laser, which allows checking for excessive background signal and PMT instability. Also, a "balance test" was added that occurs 1 second after each laser shot. A light-emitting diode produces a signal much stronger than the background light in both PMT channels during receiver operation. (A mechanical shutter at the telescope output allows complete cutoff of the background light if desired.) The ratio of the two signal channels checks the gain balance of the PMT's.

The silicon photodetector, as previously noted, is used to detect the Rayleigh-Mie return. Initially, this signal will be used to check alinement of the laser and receiver and to detect returns that would overload the rest of the receiver. The Rayleigh return signal in combination with the Raman returns can be used to obtain gas composition data. Because the Rayleigh signal is relatively large, the silicon photodetector is better suited for this application and it is free of most of the PMT problems.

Range resolution. - Range resolution, or the effective length of the target being sensed, is another factor affecting design. Range resolution is determined by the pulse width of the laser, the pulse width of the sampling pulse, and the rise time of the detection electronics. In this system the sampling pulse width is set approximately equal to the laser pulse width, that is, 20 nanoseconds. Shorter sampling pulses reduce the effective sensitivity, and longer pulses degrade the resolution. However, sampling pulses as long as 100 nanoseconds are available by changing the delay line on the range card so that resolution can be traded for sensitivity at longer ranges. The anode rise time of the PMT's, which is about 10 nanoseconds, sets the effective signal-detection rise time. The theoretical resolution of this system with a 20-nanosecond sampling time is 3.3 meters. The 10-nanosecond signal rise time should degrade the actual resolution to about 4.7 meters for distributed targets.

Digital output. - The output format of the lidar system is also a design factor. A digital output format is convenient and easy to use in data analysis. Thus, although this lidar is basically analog, the electronics are designed to display and and record output in a digital format. The output of each Raman channel is a three-digit decimal number with 999 as full scale. The output is approximately a linear function of the PMT output current.

RECEIVER CIRCUITS

Block Diagram

The following list gives the sequence of one complete receiver cycle, including the test operations. The number of each item corresponds to the circled numbers in figure 2, which indicate the system element associated with that respective operation:

(1) The laser fires a shot.

(2) The photodiode detects the shot and starts the receiver timing cycle.

(3) The time card converts the photodiode signal to emitter-coupled logic (ECL) levels. This signal triggers a 1/2-second delay timer for the background test and a 1-second delay timer for the balance test.

(4) The laser shot signal is sent to the slow driver card, which in turn drives mechanical counters to tally shots and tests. This card also drives the light-emitting diode during the balance test.

(5) The laser shot signal is also sent to the range card, where it starts a series of timers. The first timer is set by the front panel control "gain delay"; this timer sets the delay time before the PMT is turned on. The second timer is the "range" timer which sends a sampling pulse to each sample-and-hold gate. The third timer sends an encode command to each of the analog-to-digital converters (ADC). The fourth timer sends a print command to the printer.

(6) The PMT driver card receives the output of the gain-delay timer on the range card. This logic signal is then amplified to about +100 volts and sent to both PMT's to turn them on in 270 nanoseconds.

(7) The tailgate card has a timer controlled by the front panel "tailgate" control. This timer is triggered by the laser shot signal from the time card. When this timer times out, it sends a 100-volt pulse to both PMT's to turn them off in 100 nanoseconds.

(8) The PMT blocks include networks for the high-voltage divider circuits and capacitors to couple the gain turnon and turnoff pulses to four dynodes of each tube.

(9) The current out of the PMT's is fed into 50-ohm-input, wide-band amplifiers. The amplifiers are direct coupled, with an upper frequency cutoff of about 200 megahertz. The voltage gain in each amplifier can be set between 1 and 10. Two amplifiers may be cascaded in each Raman channel if required.

(10) The amplifier output is limited to -1.3 volts to assure proper sample-and-hold operation.

(11) The sample-and-hold gates (50-ohm input) provide an output which is a linear function of the integral of its input voltage during the time the sampling pulse is present. This output is held for 500 microseconds and then resets itself automatically to zero.

(12) The amplifier card has two operational amplifiers with voltage gain settings of 2 to 10.

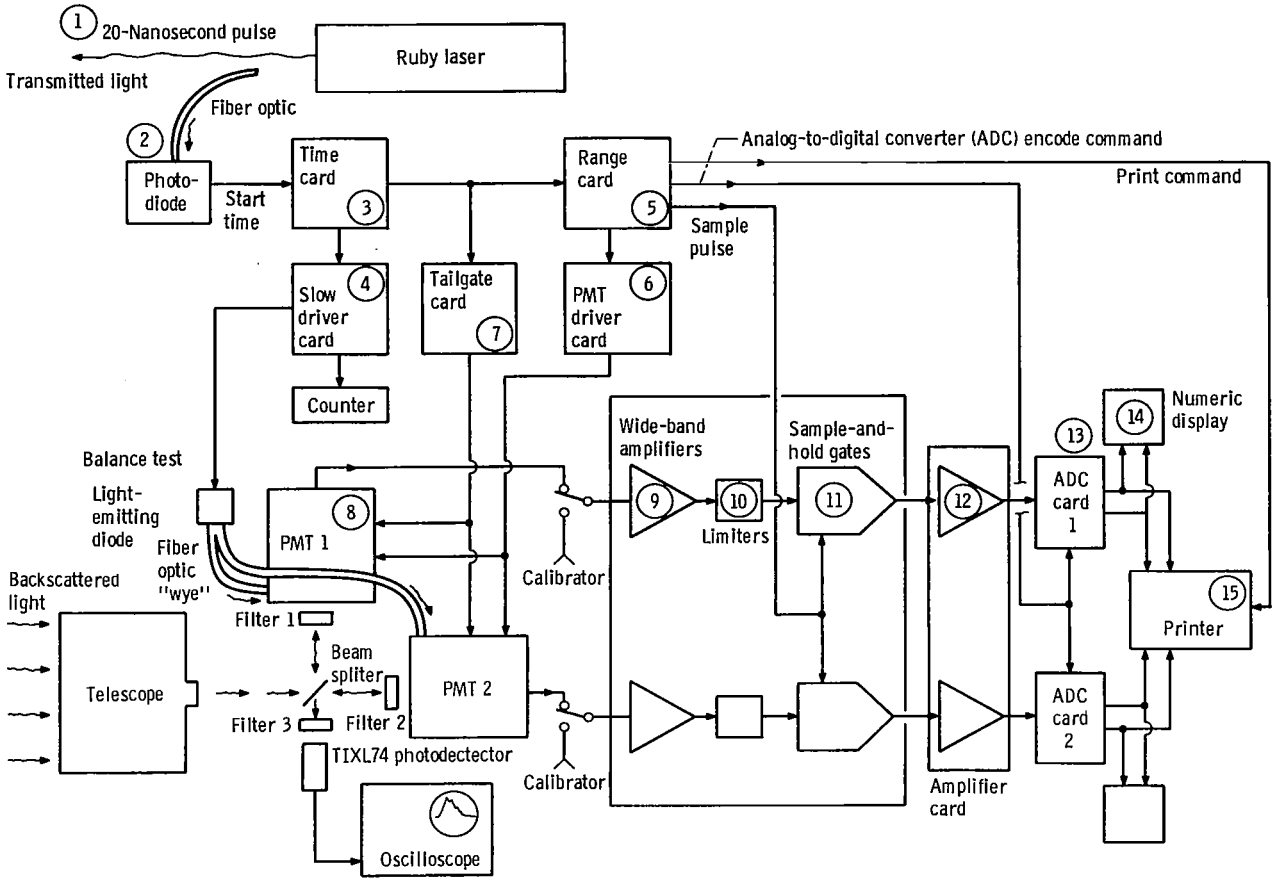

Figure 2. - Block diagram of Raman lidar.

(13) The ADC cards convert the sampled signals of each channel into 12-bit binary-coded decimal numbers.

(14) The numeric displays show the output of each ADC as a three-digit decimal number.

(15) The printer prints the outputs of both ADC's and a test identification digit on a single line.

One-half second after the laser shot, the background timer on the time card causes the receiver to operate again (steps 4 to 15). The result of this second operation is printed with a background test identification number.

One second after the laser shot the balance test timer on the time card causes the slow driver card to turn on a light-emitting diode. The light-emitting diode illuminates both PMT's through a fiber optic array. The receiver is again operated (steps 4 to 15). The printout will have a balance identification number. This test determines the ratio

of gains, or balance, of the two PMT channels. This completes one receiver cycle.

Waveforms

Typical receiver waveforms are illustrated in figure 3. Figure 3(a) shows what the PMT output of a lidar system should look like if no gain control circuits were used. Assuming the target of the lidar is clear air, the mean return is a continuous function of range with an inverse square dependence. Also shown is a potential receiver overload caused by an object in the field of view. As indicated, the PMT output fluctuates due to the low light level; that is, the number of photons being captured is few enough that the Poisson nature of the signal is a dominate feature.

The waveform shown in figure 3(b) is the PMT turnon pulse. The gain-delay control locates the pulse position. The gain-width control sets the pulse width. The tailgate pulse is shown in figure 3(c). The tailgate turns the PMT off, thus avoiding an overload from the object in the field of view. Without the tailgate the gain would not be reduced sufficiently to protect the PMT. The combined effect of the gain pulse and the tailgate pulse on the PMT output is shown in figure 3(d). The timing of the gain and tailgate pulses has thus been adjusted to prevent overload of the receiver electronics by the PMT current.

The sampling pulse from the range card is typically 20 nanoseconds wide (fig. 3(e)). This width is set by a plug-in delay line on the range card. While this pulse is present, the PMT signal is integrated by the sample-and-hold gate. The time, or range position, of this pulse is set independently of the gain controls. This allows an interval of range defined by the PMT output in figure 3(d) to be scanned by adjusting only the range control. The output circuits of the sample and hold (fig. 3(f)) require about 2 microseconds to reach steady state. The amplitude of the steady-state output is proportional to the integral of the signal during the 20-nanosecond sampling time.

Figure 3(g) shows that the ADC encode command is delayed until the sample and hold has settled. Four microseconds is required for the ADC input circuits to acquire the signal level, and 16 microseconds after encode command the digital conversion is complete. The ADC output number is held until the next receiver operation.

Circuit Details

This section considers some of the specific circuit details associated with the waveforms previously presented. A complete receiver schematic is included in the appendix.

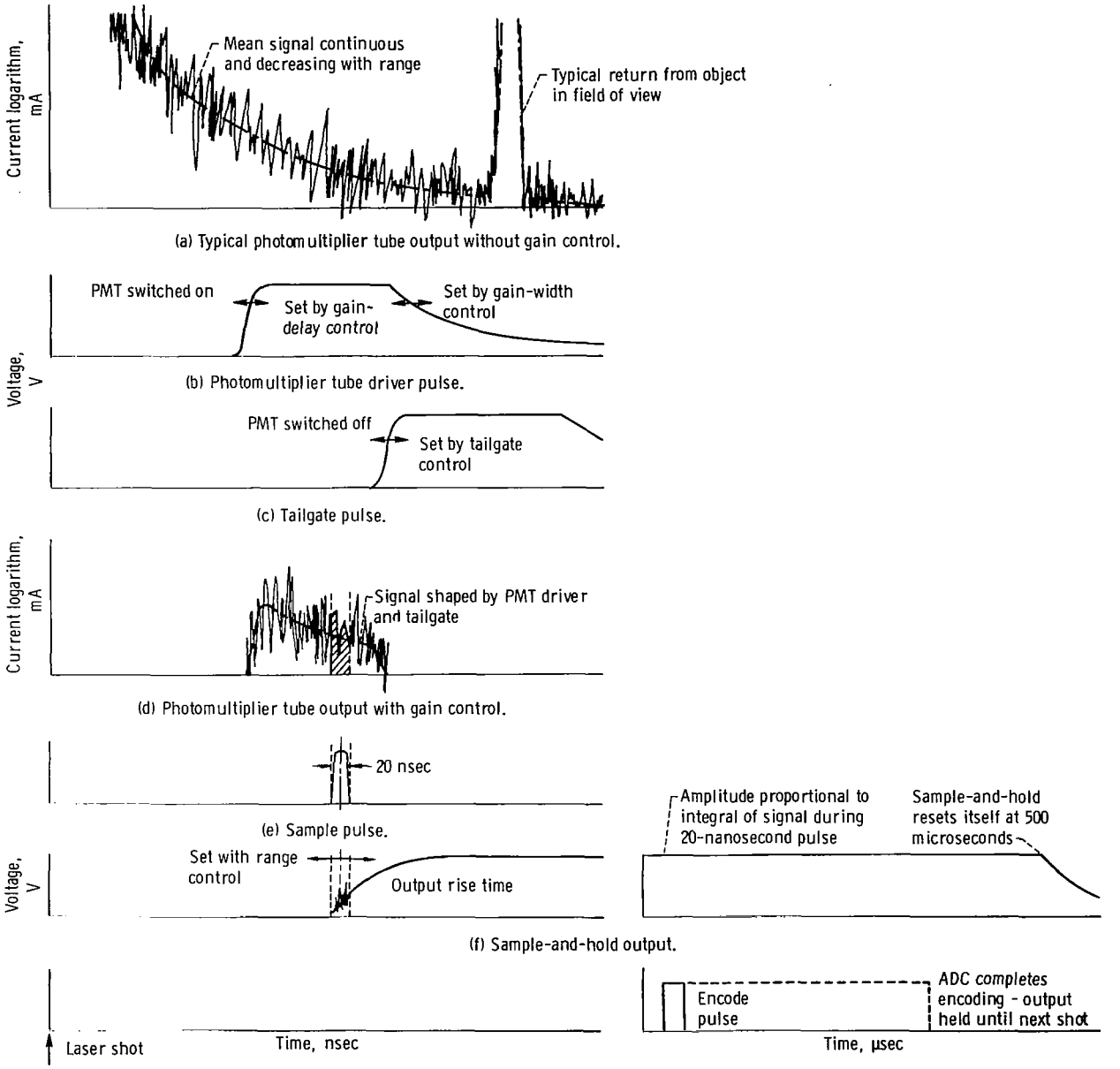

Figure 3. - Illustration of receiver waveforms.

However, in this section only the gain control, the range card, and the digitizing circuits will be examined.

Gain control circuits. - As previously noted, the objective of these circuits is to switch the gain rapidly from a low quiescent value to a high value after recovery from an optical overload condition. Electrical gain control utilizes the dynode-voltage-versus-gain characteristics shown in figure 4 for four types of dynode construction. The dynode pulse is picked to be about the same as the normal voltage between adjacent dynodes. The PMT's selected for this receiver are EMI-type 9658RM tubes with venetian blind dynodes. Venetian blind dynodes have the advantage that near the normal operating voltage the gain is not sensitive to small variations in dynode voltage. One disadvantage of these dynodes is that a large voltage pulse is needed for a modest gain change. A

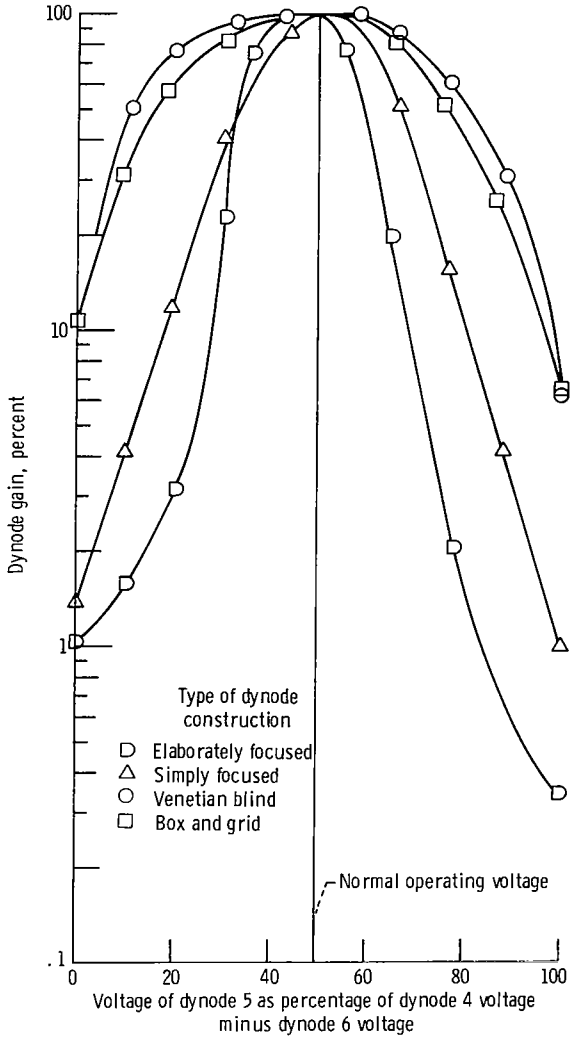

Figure 4. - Dynode gain as function of voltage (commercial data).

second disadvantage is the reduced bandwidth of the PMT, which reduces the range resolution. The gain voltage can be applied to every other dynode if the voltage per dynode of the tube is constant. Since most PMT's use a higher voltage per dynode at the anode end of the tube, about one-third of the dynodes are normally available for gain control. A gain reduction of about tenfold should be achieved for each dynode which is controlled.

The gain control network, shown in figure 5, has a direct-coupled voltage divider to supply the PMT cathode, dynode, and anode voltages. This divider circuit is through D1, R3, R6, R9, R12, R15, R16, and R17. Notice that dynode pairs 2 and 3, 4 and 5, 6 and 7, and 8 and 9 are effectively connected together; this sets the low quiescent gain. The gain network also has two capacitor-coupled circuits for application of the voltage pulses to the dynodes. The first circuit is for the voltage pulse to dynodes 3, 5, 7, and 9 to increase the gain. A typical dynode circuit for increasing the gain is C5 to R5 to C9 to the coax return, in which the pulse voltage across R5 increases the gain. The second capacitor circuit is for the tailgate pulse. A typical circuit for decreasing the

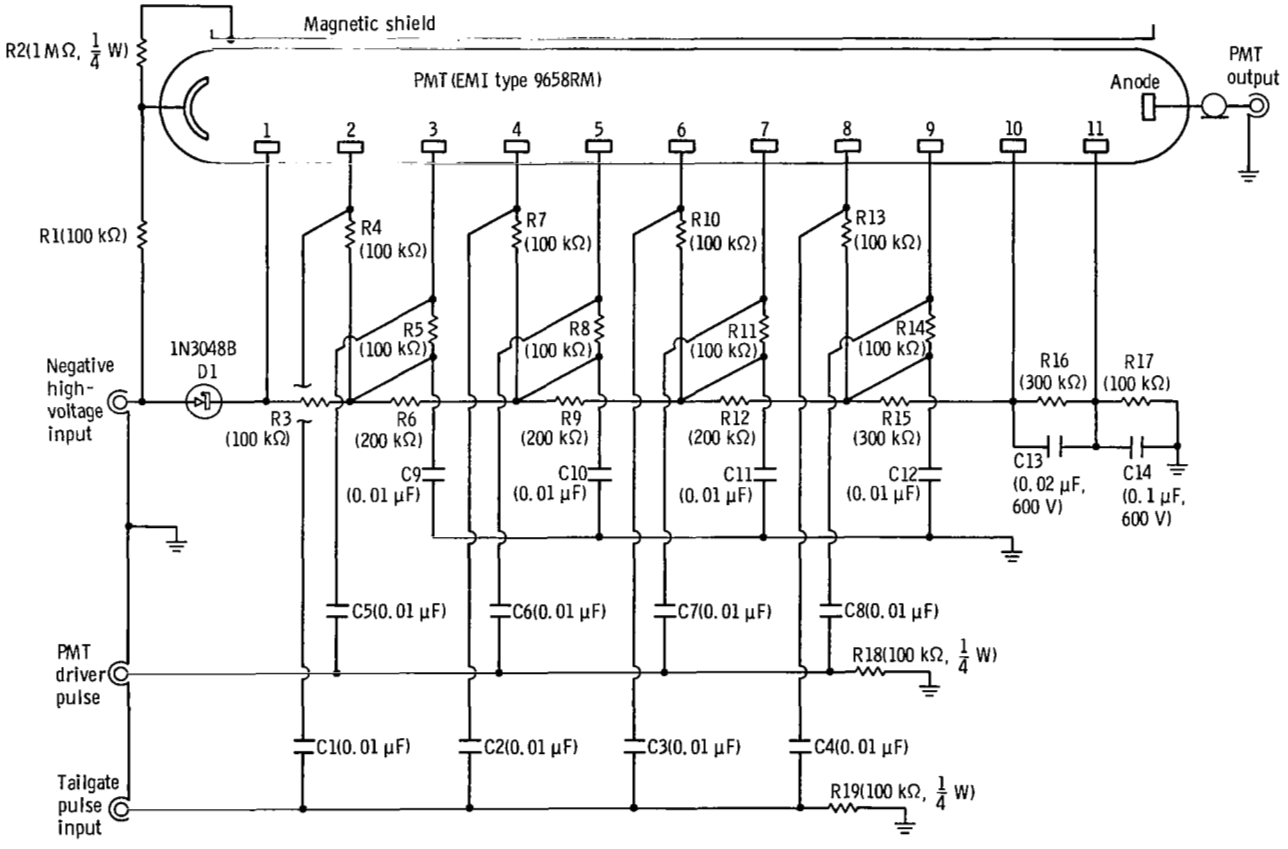

Figure 5. - Photomultiplier gain control network. (All 0.01-μF capacitors rated 3 kV; all resistors 1/2 W, 1 percent; metal film except as noted.)

gain is C1 to R4 to C9 to the coax return. The pulse voltage across R4 reduces the gain.

Due to wiring and tube capacitance, the voltage-pulse rise and fall transients induce some transients in the tube output. By limiting the rise time to not less than 180 nanoseconds, these transients are low and decay to zero before the flat-top portion of the pulse occurs. No special care was taken to minimize lead lengths or to shield components since most of these transients are generated and coupled inside the tube.

Another portion of the gain control network is the PMT driver card, which generates the voltage pulse for gain control. The PMT driver card shown in figure 6 converts the

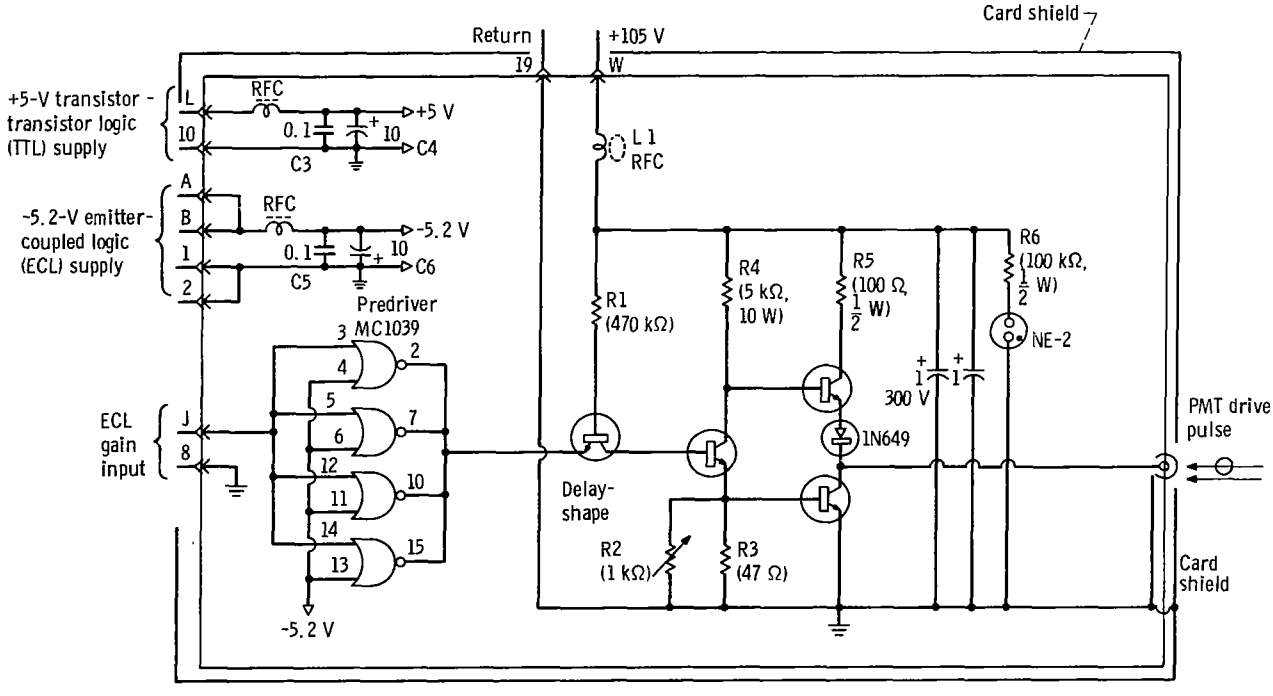

Figure 6. - Photomultiplier tube driver card. (All capacitors in μF.)

logic input into a +100-volt flat-top pulse to drive the PMT gain control network. A standard transistor - transistor logic (TTL) "totem pole" circuit generates the 100-volt output pulse. This circuit has an inherent settling time of about 200 nanoseconds due to switching times of the medium-high-voltage transistors used. The switch-on delay and pulse shape are adjustable over a moderate range by the "delay-shape" trimmer. The output pulse is coupled to the PMT gain network by high-impedance coax to keep the capacitive loading down to a reasonable value.

The emitter-coupled logic (ECL) input is converted to TTL by four paralleled gates.

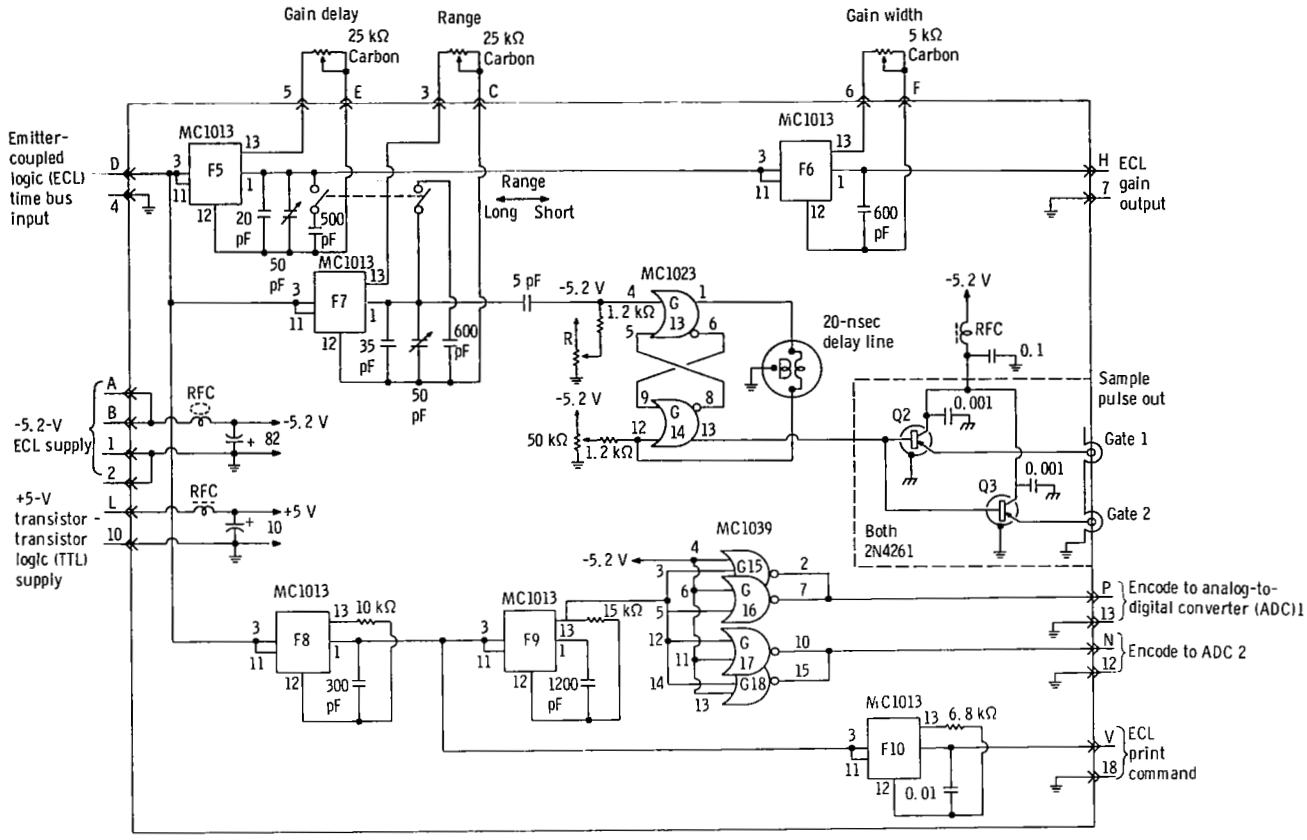

Figure 7. - Range card. (All capacitors in μF unless noted.)

The parallel operation reduces the delay of the output pulse. Since the PMT driver card generates transients, it is necessary to isolate it from other circuits. The circuit card is decoupled from the +105-volt supply by L1, C1, and C2. The decoupling prevents noise coupling to other logic circuits. For the same reason the whole card is shielded. All shields in the receiver are connected to facility ground.

Range card. - The components of the range card are shown in figure 7, and the functions are described in table I. The basic timer circuit used throughout the receiver is a simple monostable multivibrator built with MC1013 flip-flops. The circuit is shown in figure 8. The circuit is used for delays from 50 nanoseconds to 1 second. The time delay is adjustable if a low-inductance, variable resistor is used for R. This circuit is used for all the timers on the range card except for the sampling pulse.

The timer for the sampling pulse is a delay-line monostable multivibrator. The delay line is important in stabilizing the pulse width since the receiver sensitivity is di-

TABLE I. - RANGE CARD FUNCTIONS

Functions	Components
Timer to delay turnon of photomultiplier tube (PMT) gain	F5
Timer to control on-time of PMT gain	F6
Timer to set range at which data are taken	F7
Delay-line monostable multivibrator to generate sampling pulse for sample-and-hold gates	G13, G14, Q2, Q3
Timer to delay analog-to-digital converter (ADC) encode signal	F8, F9
Convert ADC encode signal to transistor - transistor logic (TTL) encode command	G15, G16, G17, G18
Timer to delay emitter-coupled logic (ECL) print command	F8, F10

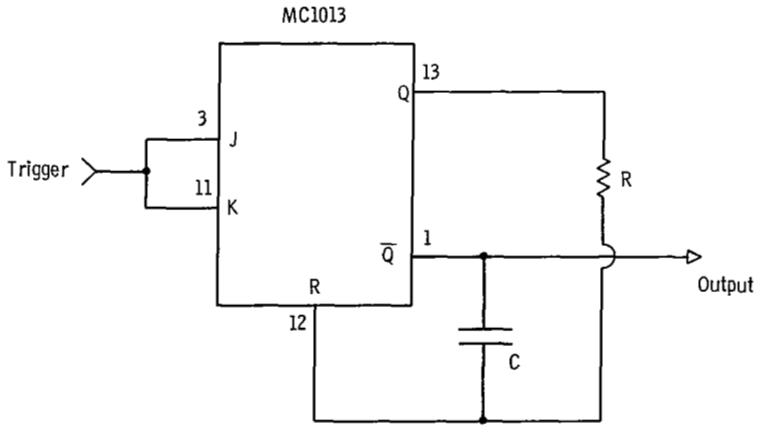

Figure 8. - Monostable multivibrator. Time ≈ 1.4 RC; 1 kΩ < R < 100 kΩ.

rectly proportional to the pulse width. The basic circuit is shown in figure 9 (ref. 14). A set of plug-in delay lines covering the range of 10 to 100 nanoseconds is used. The delay lines are twisted-pair wire type. Adjustment of the two variable resistors gives control over pulse shape and width.

The base-emitter voltage drop of the gate driver transistors Q2 and Q3 (fig. 7) converts the -0.75-volt to -1.50-volt signals to the 0-volt to -0.7-volt pulses that gate the sample-and-hold units. Because the gate operation is not sensitive to the amplitude of the gating pulse, this method is satisfactory.

Digitizing circuits. - The most critical component involved in digitizing the signals is the sample-and-hold gate. The gate is a standard nuclear instrumentation module called a "linear gate and hold" by its manufacturer. This gate has a 100-megahertz

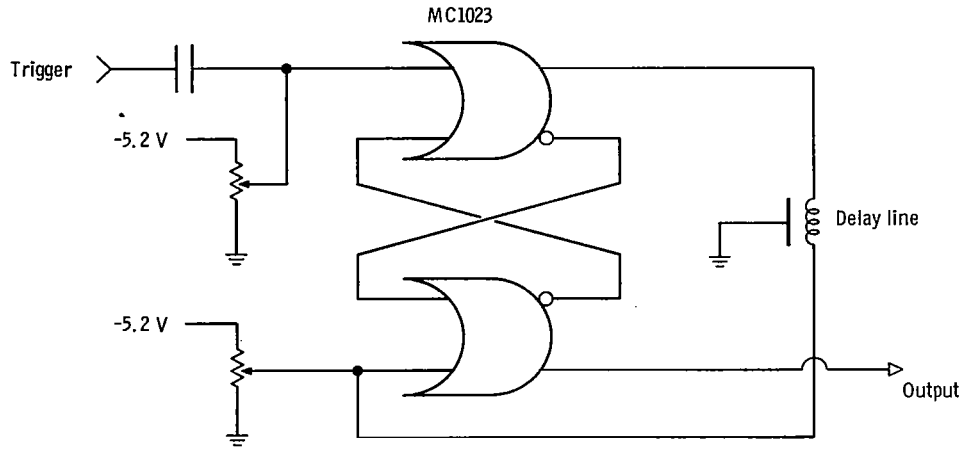

Figure 9. - Delay-line monostable multivibrator.

analog bandwidth and a combined gate opening and closing time of 5 nanoseconds. The gate output can be monitored with a sampling oscilloscope. The gate output is integrated and held such that the magnitude of the output is a linear function of the integral of the signal during the gate opening. The output has a settling time of about 2 microseconds. The output drops less than 1/2 percent during the 500 microseconds that the output is held.

The remainder of the digitizing circuitry is composed of moderate-speed commercial units - ADC's with a 20-microsecond cycle time, light-emitting-diode numeric displays, and a printer. The ADC's are 12-bit binary-coded decimal units that give three-decimal-digit output per Raman channel. All the digital circuits are TTL compatible.

PERFORMANCE

The assembled circuits were mounted in the lidar receiver rack shown in figure 10. In order to provide for bench testing of the completed receiver with a simulated lidar signal, a breadboard PMT mount was constructed, as shown in figure 11. This PMT mount contains two EMI 9658RM photomultiplier tubes and a TIXL74 silicon photodetector module. In these tests no optical filters are used with the detectors. The lidar signal is simulated by illuminating the end of the mount opposite the detectors with a light-emitting diode. The light-emitting diode is driven by a pulse generator. Receiver controls are adjusted for proper timing by driving the "start time" input of the time card with a second pulser synchronized to the light-emitting-diode pulser. The switch on the time card (see appendix) is set to "adjust," which shortens the delay of the back-

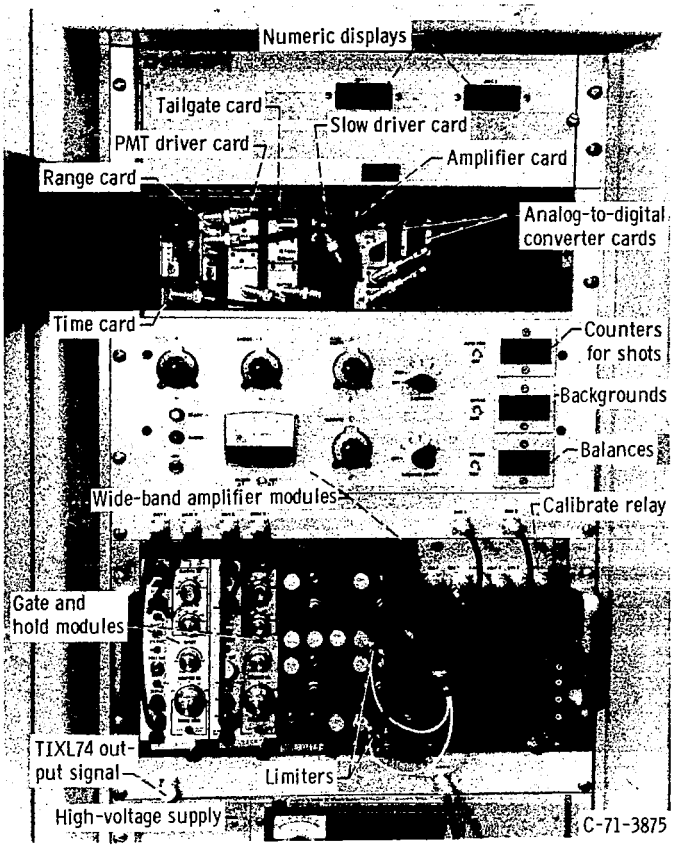

Figure 10. - Lidar receiver rack.

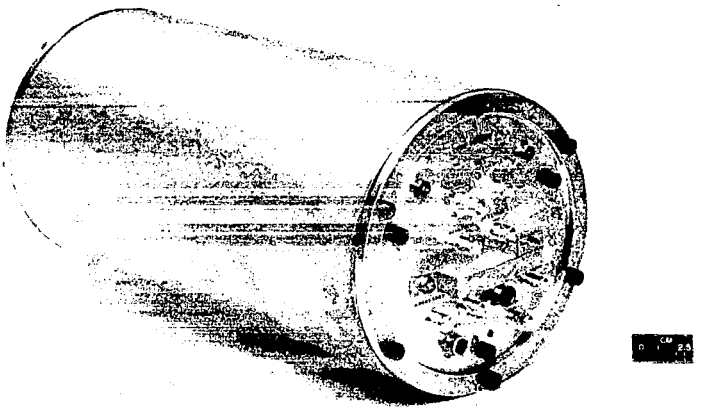

C-71-3542

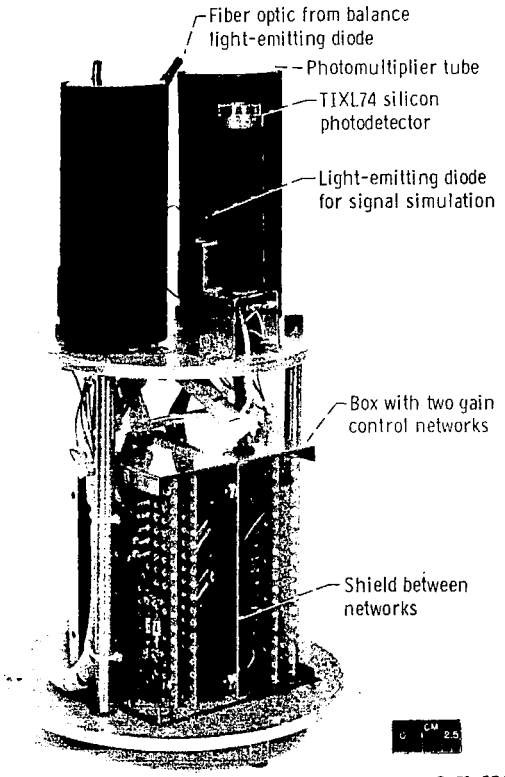

C-71-3541

Figure 11. - Breadboard photomultiplier tube mount.

ground and balance tests so that the receiver may be cycled at 5 kilohertz. The waveforms of the receiver can then be observed as repetitive traces. The gain delay, gain width, range, and tailgate can then be set by using the oscilloscope time base.

The warmup drift of the digital zero is about +40 counts (999 counts full scale) in 30 minutes. Most of this drift is traceable to the wideband amplifiers and the sample-and-hold gates. Since the background and balance tests are performed after each shot and used to correct the data, this slow drift does not reduce the accuracy of the system.

Operation

Typical data obtained during operation of the lidar receiver unit and the breadboard PMT mount are shown in figure 12. The waveforms of figure 12(a) show the gain control pulse, the sampling pulse, and the photomultiplier tube output. A relatively intense light was used so that noise would not obscure the PMT output waveform. The PMT's are pulsed with 100 volts per dynode for both the gain and tailgate pulses. The measured

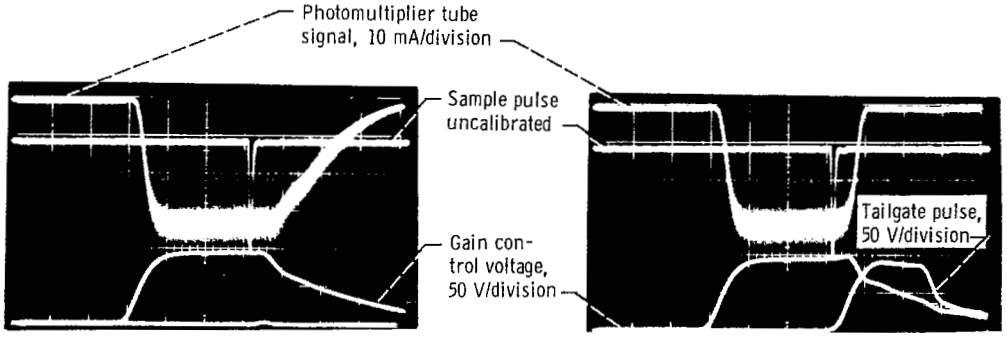

Time, 200 nsec/division

(a) Photomultiplier tube gain control without tailgate pulse.

(b) Photomultiplier tube gain with tailgate pulse.

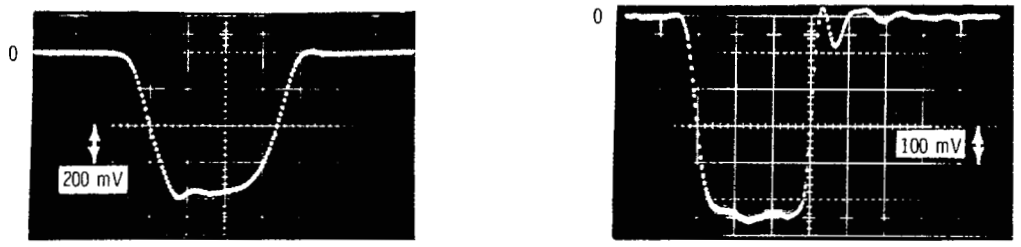

Time, 5 nsec/division

(c) Sampling pulse from range card.

(d) Fast gate output of sample and hold.

Figure 12. - Gain and sampling waveform data.

gain reduction is about fifteenfold per dynode controlled, so that the total gain control with four dynodes is about 50 000-fold. Due to the deadtime of the PMT driver card, the PMT will not begin to turn on during the first 50 meters of range. No afterpulsing was observed during this bench testing, but actual field testing is necessary before its presence or absence can be fully evaluated.

Figure 12(b) shows the effect of the tailgate pulse on the PMT output. The gain turnoff has been reduced to less than 200 nanoseconds, or 30 meters of range. The sampling pulse is positioned to show that data could possibly be obtained as close as 30 meters from an object producing receiver overloads.

Figure 12(c) shows the sampling pulse to the sample-and-hold gate. The delay-line monostable multivibrator produces a 18-nanosecond-wide pulse at one-half amplitude and a -0.7-volt peak into 50 ohms. The fast output of the sample-and-hold gate is shown in figure 12(d). This shows the actual switching of the linear sampling gate. The linear-gate-and-hold unit shortens the pulse to 15 nanoseconds of effective width and improves the waveform. It was experimentally verified that the output of the gate is directly proportional to the effective pulse width.

The receiver sensitivity was checked by feeding a calibrated current into the input of each wide-band amplifier. With a delay line giving 20 nanoseconds effective width, 27.3 milliamperes input at low gain will give full-scale output (999). At high gain, 0.575 milliampere will give full-scale output. Other sensitivity ranges could be obtained with another wide-band amplifier or attenuation. The 0.575-milliampere full-scale output corresponds to a 1.27×10^{-5} count per photoelectron (during a 20-nsec sample). This implies, when using the PMT vendor-supplied information (i.e., a current gain of 2×10^{6} and a quantum efficiency of 8.1 percent at 694.3 nm), a system sensitivity of 2.5 counts per signal photon.

Noise Tests

Many lidar receivers have had development problems with laser electrical noise (ref. 15). Apparently, the most troublesome noise source is the laser Q-switch. The laser to be used with this receiver has a Q-switch thyratron which switches 15 kilovolts at a peak current of about 300 amperes. Because the ECL logic family used in the receiver has a noise margin of only 350 millivolts or less, noise was a consideration in the design and testing of this system.

The receiver circuits are protected from noise by powerline and internal filtering, low inductance grounding, and shielding. The powerline is brought into the receiver rack through an EMI filter and a constant-voltage transformer. The internal filtering consists of EMI filters on all dc power supply outputs and decoupling of circuit card

power loads. The shielding includes the use of shielded wire for critical logic signals and metal flex hose for external cable shielding.

The receiver was set up next to the laser, with the layout and cable length selected to simulate the final installation. The fiber optic for the receiver timing signal (fig. 1) was disconnected. A series of laser shots at various energies were run. The receiver did not trigger, showing that induced noise would not cause false triggering. Another series of shots were run with the fiber optic connected and adjusted for proper triggering. The noise pickup in the Raman channels was measured as less than 0.03 percent of full scale with the receiver adjusted for maximum gain.

CONCLUDING REMARKS

Bench testing of the receiver has shown that it should successfully cope with known lidar problems. Standard lidar problems include photomultiplier tube (PMT) instability and overload, conversion of the PMT signal to numerical data, diagnostic testing methods, and laser-induced electrical noise. The gain control network, the PMT driver card, and the tailgate card can provide a 50 000-fold gain reduction during possible optical overloads to protect the unstable PMT's. Further stability is obtained with thermal insulation to minimize temperature changes. A well-regulated high-voltage supply common to both signal channels controls the voltage sensitivity of the gain.

The diagnostic features, the background and balance tests, permit confidence checks of PMT operation, background light interference, and gain stability. Another diagnostic feature is the Rayleigh-Mie detector. The silicon detector for the Rayleigh-Mie return provides a third independent check of the signal for overload conditions. The silicon detector, which is intrinsically more stable than PMT's, will help check alinement of the laser and receiver optics.

Many data reduction problems are bypassed by recording the data in digital form rather than recording by an oscilloscope camera. The two Raman channels are digitized by moderate-speed commercial analog-to-digital converters, numeric displays, and a printer.

The fast sample-and-hold unit has demonstrated its ability to handle 20-nanosecond samples of PMT signal. The resulting range resolution is expected to be less than 5 meters for the complete lidar system. The sampling process and the other electronic functions have been demonstrated to operate reliably without any problems from laser-induced noise.

Lewis Research Center,
National Aeronautics and Space Administration,
Cleveland, Ohio, April 11, 1972,
113-31.

APPENDIX - ELECTRICAL DIAGRAM

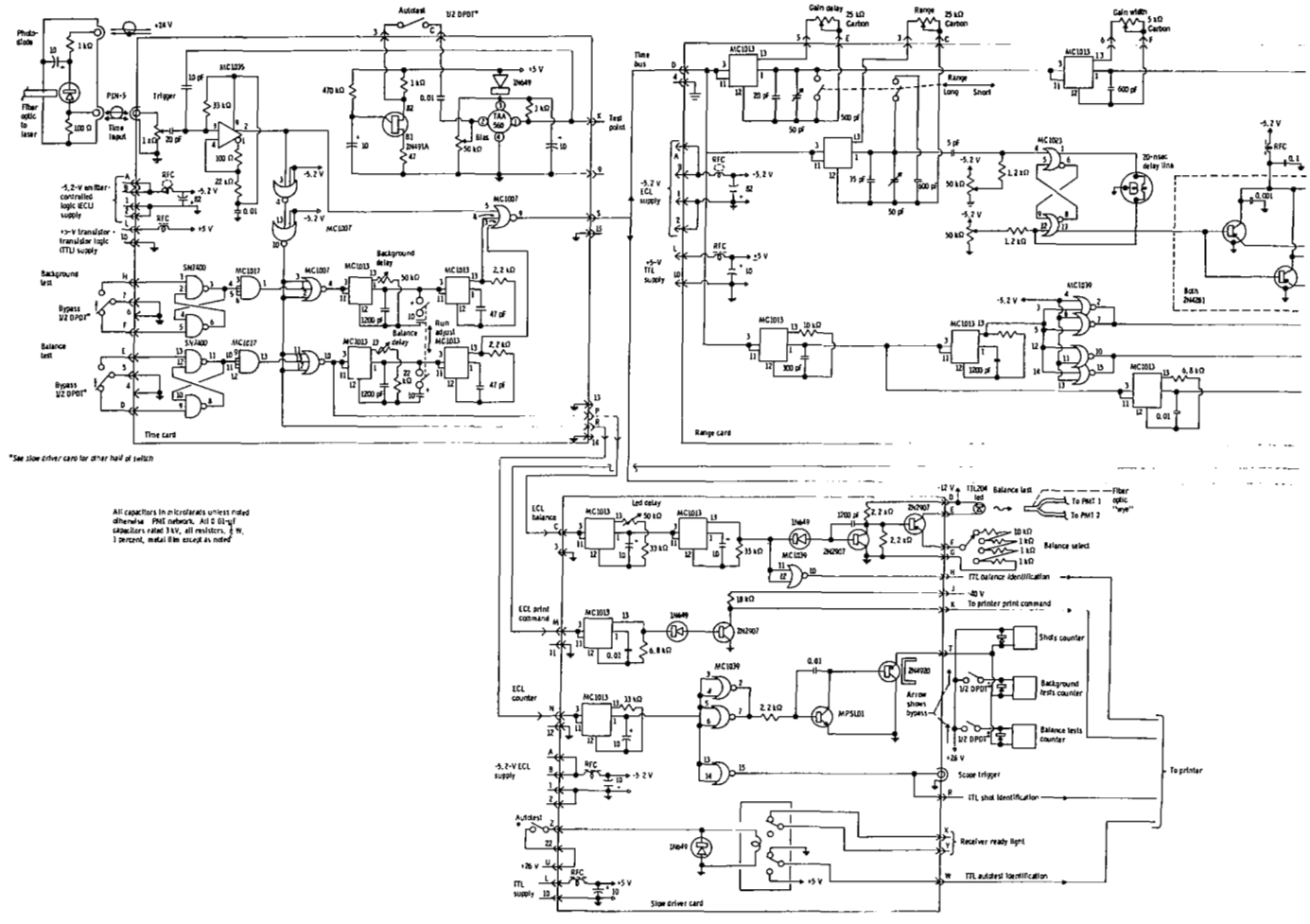

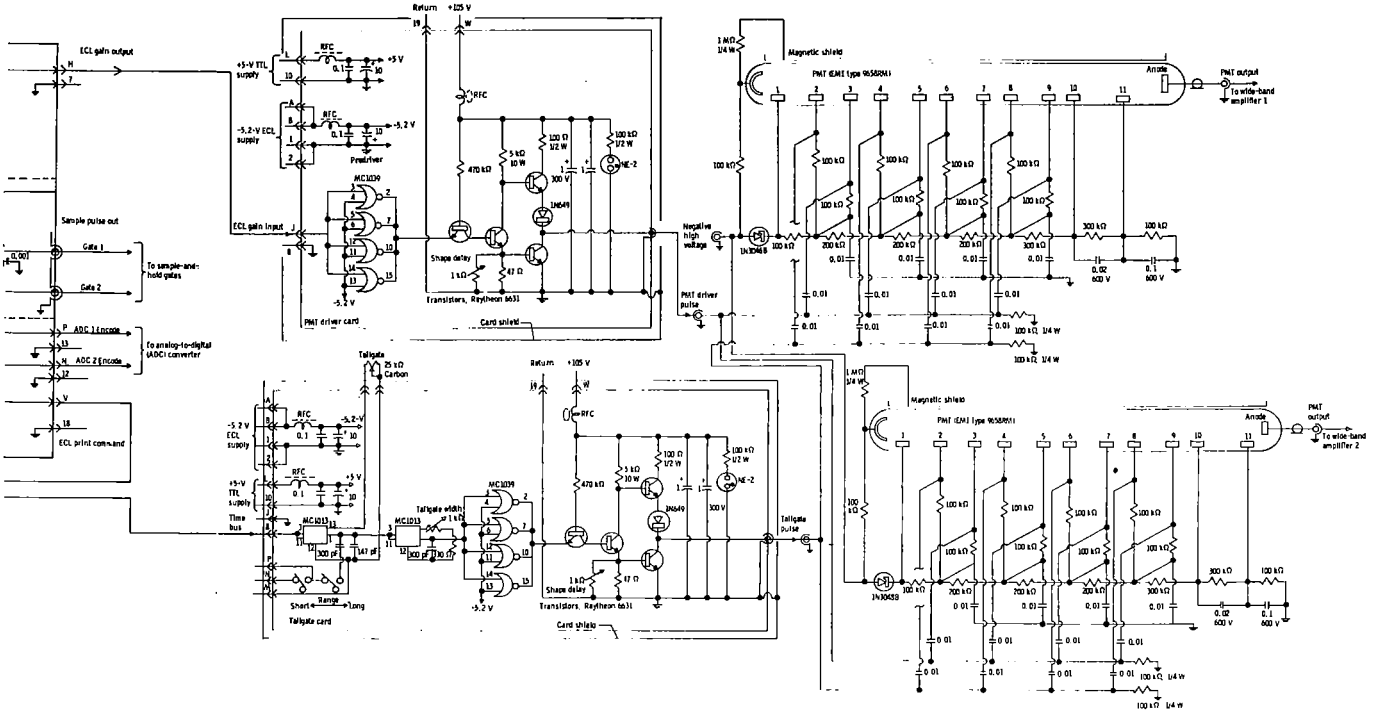
ECL gain output
Sample pulse out
Gate 1
Gate 2
To sample-and-hold gates
To analog-to-digital (ADC) converter
ECL print command
+5-V TTL supply
-5.2-V ECL supply
Pretriver
ECL gain input
MC1039
PMT driver card
Return +105 V
RFC
470 kΩ
5 kΩ 10 W
100 Ω 1/2 W
100 kΩ 1/2 W
300 V
1N649
Shape delay
1 kΩ
47 Ω
Transistors, Raytheon 6631
Card shield
Negative high voltage
1N3048
PMT driver pulse
1 MΩ 1/4 W
Magnetic shield
PMT (EMI type 9658RM)
Anode
PMT output
To wide-band amplifier 1
100 kΩ
200 kΩ
300 kΩ
0.01
0.02 600 V
0.1 600 V
100 kΩ 1/4 W
Tailgate
25 kΩ Carbon
-5.2 V ECL supply
+5-V TTL supply
Time bus
MC1013
Tailgate width
1 kΩ
300 pF
147 pF
30 pF
Short
Range
Long
Tailgate card
Tailgate pulse
PMT output
To wide-band amplifier 2

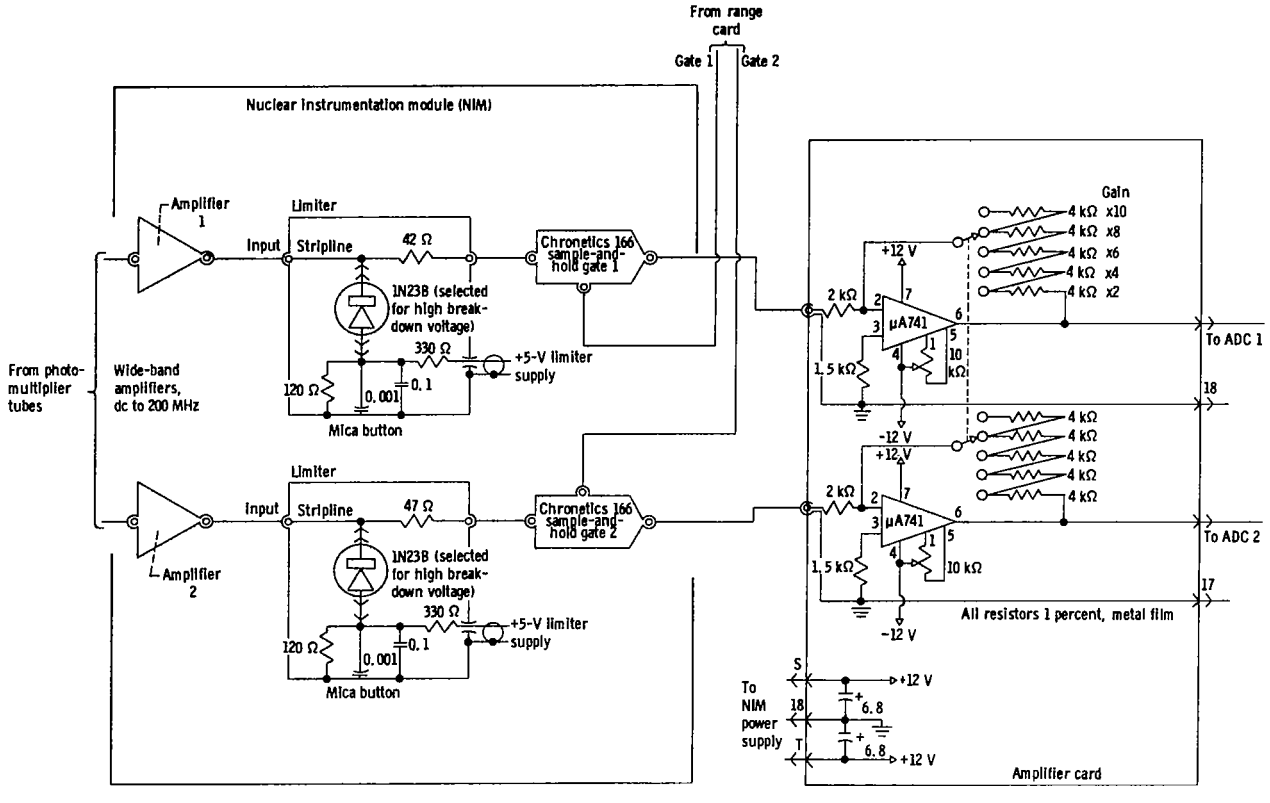
From range card
Gate 1
Gate 2
Nuclear instrumentation module (NIM)
Amplifier 1
Limiter
Input
Stripline
42 Ω
Chronetics 166 sample-and-hold gate 1
1N23B (selected for high breakdown voltage)
330 Ω
+5-V limiter supply
120 Ω
0.001
0.1
Mica button
From photomultiplier tubes
Wide-band amplifiers, dc to 200 MHz
Amplifier 2
47 Ω
Chronetics 166 sample-and-hold gate 2
Gain
4 kΩ x10
4 kΩ x8
4 kΩ x6
4 kΩ x4
4 kΩ x2
+12 V
2 kΩ
μA741
1.5 kΩ
10 kΩ
To ADC 1
18
-12 V
4 kΩ
To ADC 2
17
All resistors 1 percent, metal film
S
To NIM power supply
6.8
T
Amplifier card

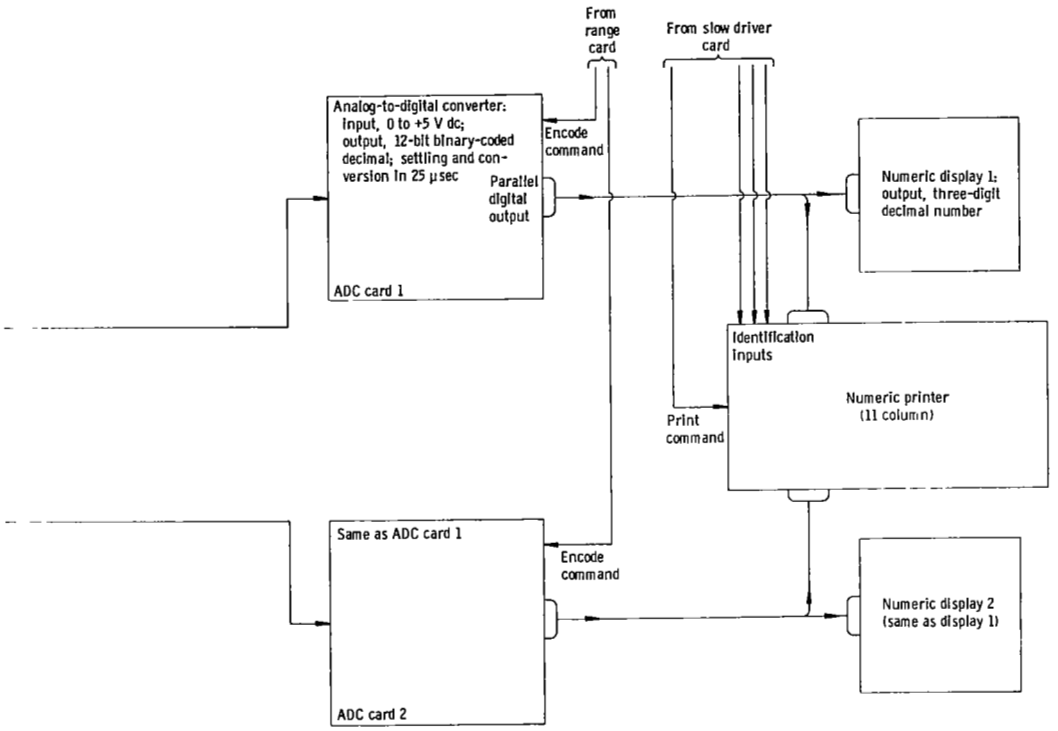
From range card
From slow driver card
Analog-to-digital converter: input, 0 to +5 V dc; output, 12-bit binary-coded decimal; settling and conversion in 25 μsec
Encode command
Parallel digital output
ADC card 1
Numeric display 1: output, three-digit decimal number
Identification inputs
Numeric printer (11 column)
Print command
Same as ADC card 1
Encode command
Numeric display 2 (same as display 1)
ADC card 2

REFERENCES

1. Derr, V. E.; and Little, C. G.: A Comparison of Remote Sensing of the Clear Atmosphere by Optical, Radio, and Acoustic Radar Techniques. Appl. Opt., vol. 9, no. 9, Sept. 1970, pp. 1976-1992.

2. Collis, R. T. H.: LIDAR. Advances in Geophysics. Vol. 13. H. E. Landsberg and J. Van Mieghem, eds., Academic Press, Inc., 1969, pp. 113-139.

3. Evans, W. E.; and Collis, R. T. H.: Meteorological Applications of Lidar. S.P.I.E.J., vol. 8, Jan. 1970, pp. 38-45.

4. Leonard, Donald A.: Observation of Raman Scattering From the Atmosphere Using a Pulsed Nitrogen Ultraviolet Laser. Nature, vol. 216, Oct. 14, 1967, pp. 142-143.

5. Melfi, S. H.; Lawrence, J. D., Jr.; and McCormick, M. P.: Observation of Raman Scattering by Water Vapor in the Atmosphere. Appl. Phys. Letters, vol. 15, no. 9, Nov. 1, 1969, pp. 295-297.

6. Klainer, Stanley M.; Hirschfeld, Tomas; and Schildkraut, E. Robert: The Detection of Toxic Contaminants in the Atmosphere Using Single Ended Remote Raman Spectrometric Techniques. Presented at the Central States Section of the Combustion Institute, Houston, Texas, Apr. 7-8, 1970.

7. Cooney, John: Satellite Observations Using Raman Component of Laser Backscatter. Proceedings of the Symposium on Electromagnetic Sensing of the Earth from Satellites. Ralph Zirkind, ed., Polytechnic Institute of Brooklyn Press, 1967, pp. P1-P10.

8. Pressman, J.; Schuler, C.; and Wentink, J.: Study of Theory and Applicability of Laser Technique for Measuring Atmospheric Parameters. Rep. GCA-TR-68-6-N, GCA Corp. (NASA CR-86134), Oct. 1968.

9. Salzman, Jack A.; Masica, William J.; and Coney, Thom A.: Determination of Gas Temperatures from Laser-Raman Scattering. NASA TN D-6336, 1971.

10. Northend, C. A.; Honey, R. C.; and Evans, W. E.: Laser Radar (Lidar) for Meteorological Observations. Rev. Sci. Inst., vol. 37, no. 4, Apr. 1966, pp. 393-400.

11. McCormick, Paul D.; and Hultquist, H. David: An Atmospheric Lidar Data-Acquisition System Using an On-Line Digital Computer: Report of the Mount Haleakala Observatory. Rep. 1386-29-T, Michigan Univ. (AS-701335), Feb. 1970.

12. Anon.: RCA Phototubes and Photocells. Technical Manual PT60, Radio Corporation of America, 1963.

13. Krishnaw, Damala S.; Evans, William E.; Honey, Richard C.; and Sorenson, Glenn P.: Development of a Turbidity-Measuring Underwater Optical Radar System. Stanford Research Institute, (AD-701416), Dec. 1969.

14. Anon.: High Speed Monostable Multivibrators Design with MEC1 Integrated Circuits. AN-418, Motorola Semiconductor Products.

15. Kent, G. S.; Sandland, P.; and Wright, R. W. H.: A Second-Generation Laser Radar. J. Appl. Meteorol., vol. 10, June 1971, pp. 443-452.